JLAB-TN-21-018

THOMAS JEFFERSON NATIONAL ACCELERATOR FACILITY
12000 Jefferson Avenue
Newport News, VA 23606

Tech Note Number:
MEG0002021-R001 REV-

TITLE: THE DESIGN REPORT OF MHD STEERING CORRECTOR MAGNET IN THE CEBAF 200 keV INJECTOR BEAMLINE

BY: Seetha-Lakshmi Lalitha

DATE: 04 /26 /2021

Approver: Joe Grames

-	The initial release	04/26/2021
REV.	DESCRIPTION	DATE
SUMMARY OF CHANGES FROM PREVIOUS REVISION:		

Contents

The Design Report of MHD Steering Corrector Magnet in the CEBAF 200 keV Injector Beamline

1 Introduction

This document presents the (a) design and analysis results of the new MHD type air-core copper steering corrector magnet, (b) the manufacturing and assembly details, (c) the coil quality check and magnet performance test plan, and (d) results of magnetic performance validation analysis using the as-built coil parameters. The CEBAF 200 keV injector line [1] consists of two MHD-type magnets as shown in Figure 1.

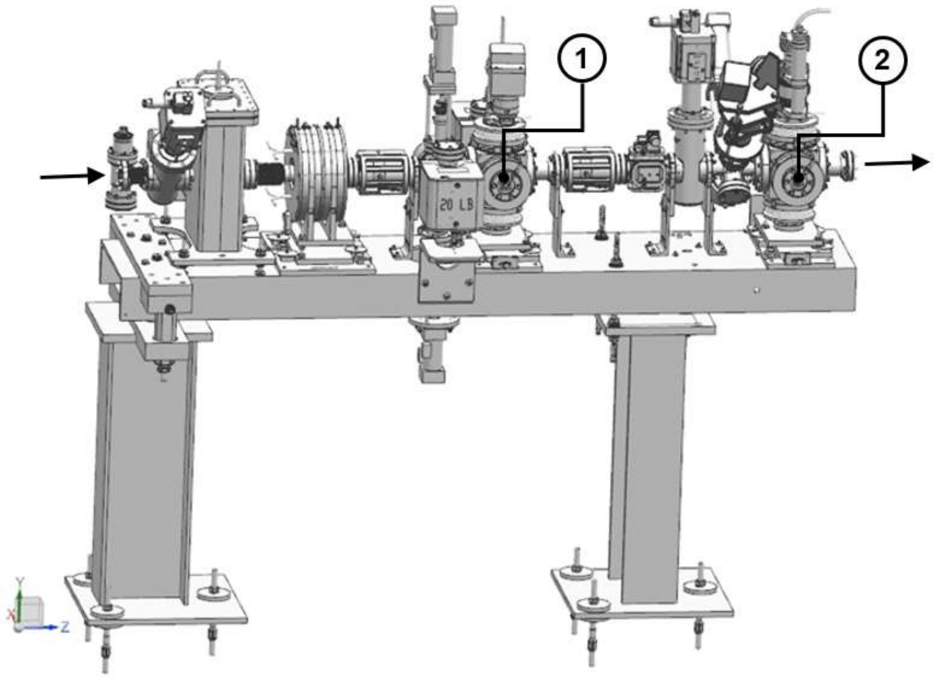

Figure 1: The aperture girder assembly in the CEBAF 200 KeV injector beamline [2]. Labels 1 and 2 denote respectively the MHD steering corrector magnet mounted onto A1 and A2 aperture cube assemblies. The arrows indicate the direction of the beam. The A1 and A2 aperture control the injector acceptance.

2 Overall Requirements

2.1 The new steering corrector magnet for the A1 and A2 aperture cube assemblies needs to be identical in design and performance.

2.2 MHD magnet entails two identical and independently energized dipole coil assemblies to provide the vertical and horizontal steering correction as needed for the beam transport.

2.3 The horizontal and vertical dipole assemblies, when energized separately, must provide a maximum integrated field strength of 5.5×10^{-5} T.m (55 Gauss-cm).

2.4 The allowable fringe field and magnetic homogeneity requirements are not specified.

2.5 Because of the overall space constraints and also to support the mechanical integration of the vacuum and beam diagnostics components on the same assembly, the electromagnetic-mechanical design for the new MHD magnet is required to be such that the coil packs can be mount directly onto the CF six-way cross cube fitting for the A1 and A2 apertures.

2.6 The allowable footprint for the new MHD magnet-aperture cube assembly remains the same as that of its predecessor in the 100 keV injector beamline.

2.7 All components used in the magnet must withstand a maximum of 200 C to comply with the bake-out procedure for the beamline vacuum components.

3 Design and Analysis Approach

The three-dimensional (3D) design for the coil and coil support structure follows the magnetic performance, mechanical assembly, and system integration requirements listed in section 2 of this document. Given the limited space available for the coils and the support structure, pancake coil geometry is found appropriate for the compact design for the magnet.

The electromagnetic (EM) design model is built using the Siemens NX CAD software package (Ver.12) through an iterative process. This model is built in the Cartesian coordinate system with the positive Z-axis (longitudinal axis) pointing in the beam direction, the Y-axis along the vertical direction, and the X-axis pointing radially outwards. The origin of the reference coordinate system coincides with the magnet center.

The 3D EM calculations were performed with the ANSYS Maxwell (Version: 2020 R2) software. The ANSYS Workbench package (Version: 2020 R2) was used for relevant multi-physics analysis to support the development of the coil and bobbin model for the baseline study. The conductor parameters and coil manufacturing aspects are appropriately integrated into the design.

The EM results reported in this document include the magnetic field characteristics, Lorentz force distribution, inductance, and stored energy. The multipole field calculations were carried out by the Fourier decomposition of the simulated field map at selected values of coil excitation currents in the range of interest. The values reported in section 7 are for a good field region (GFR) with a radius (R_{ref}) of 4 mm. The effective magnetic length (L_{eff}) of the dipole magnet and the deviation of integrated dipole field uniformity$\left(\sum_{n^*} B'_{n^*}\left(r = R_{ref}, z\right)\right)$ are given as follows:

$$L_{eff} = \frac{\int_{z=-1m}^{z=+1m} B_{n=1}\left(r = R_{ref},\ z\right).dz}{B_{n=1}\left(r = R_{ref},\ z = 0\right)} \tag{1}$$

The term in the numerator of equ.1 represents the value of the integrated strength of the leading dipole field component at R_{ref} over the Z range of $\pm$ 1 m from the magnet center ($z = 0$). The term in the denominator is the strength of the corresponding field component at the magnet center.

$$\sum_{n^*} B'_{n^*}\left(r = R_{ref}, z\right) = \sum_{n^*} \frac{\int_{z=-1m}^{z=+1m} B_{n^*}\left(r = R_{ref},\ z\right).dz}{\int_{z=-1m}^{z=+1m} B_{n=1}\left(r = R_{ref},\ z\right).dz} \tag{2}$$

where $B_{n^*}\left(r = R_{ref}, z\right)$ refers to the value of the allowed higher-order multipole field at $R_{ref}$for any given position z along the longitudinal axis of the magnet. The number n^* denotes the order of the multipole field errors.

The reported dipole integrated field quality (%) is

$$DIFQ\ (\%) = \left(1 - \sum_{n^*} B'_{n^*}\left(r = R_{ref}, z\right)\right) * 100 \tag{3}$$

The coil resistance at 20 C is calculated using the copper resistivity of 1.724×10^{-8} Ω.m.

The final 3D NX model derived from this design analysis forms the basis for the CAD drawings (see Table 3) used to manufacture the parts and the assembly of the magnet.

4 Design Description

4.1 The new MHD steering corrector magnet consists of four identical air-core pancake coils (coil-top (label 1), coil-bottom (label 2), coil-left (label 3), and coil-right (label 4) as shown in Figure 2) that form two independent dipole coil assemblies to provide beam steering correction in the vertical or horizontal direction. For example, the horizontal steering correction to the beam is achieved by the vertical dipole coil assembly with the top and bottom coils connected in series. Similarly, the horizontal dipole coil assembly of the left and right pancake coils offers the vertical beam steering correction.

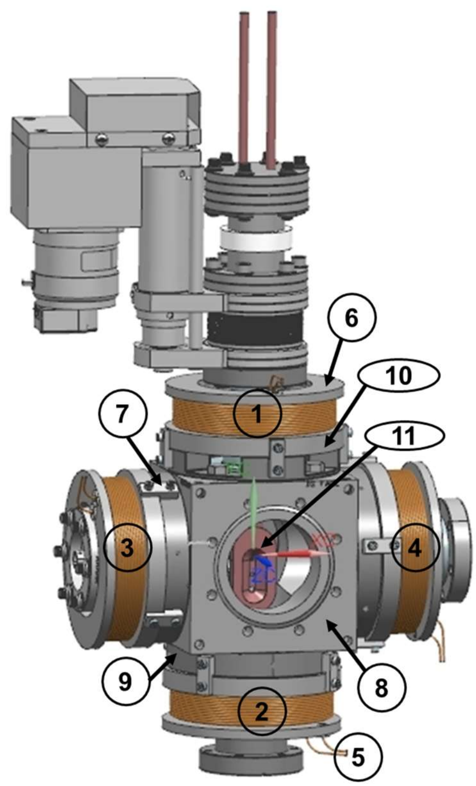

Figure 2: The MHD steering corrector magnet mounted onto the stainless-steel CF six-way cross cube [3]. The components relevant to the description in this document are MHD coil-top (label 1), MHD coil-bottom (label 2), MHD coil- left (label 3), MHD coil-right (label 4), lead wires from the MHD coil (label 5), MHD coil bobbin (label 6), magnet retaining clip (label 7), CF six-way cross cube (label 8), CF 4.5 inches OD non-rotatable blank flange (label 9), MHD mounting collar 4.5 inches OD (label 10), and A1/ A2 aperture assembly (label 11). This labeling scheme for the coils follows the assumption that the observer is facing towards the magnet assembly from the exit side of the beam.

Table 1: The design parameters of the MHD steering corrector magnet.

Part (Part number)	Parameters	Unit	Design
Magnet wire	Material, Shape		Copper; Round
	Insulation		Polyimide (Kapton)
	Bare conductor size (equivalent AWG)		14
	Diameter of bare wire, Insulated wire (maximum dimension)	mm	1.643,1.732
Coil bobbin (JL0091130-0318-01)	Material		SS 304
	Inside diameter, outside diameter of the bobbin core	mm	76.2, 82.35
	Outside diameter of the top/ bottom flange	mm	118.872
	Height of the top flange, bottom flange	mm	6.35, 12.7
	Overall height of the coil bobbin	mm	41.57
	Diameter of the opening on the top flange for the lead wires	mm	6.35
Coil (JL0091130-0318-03)	Material		Copper
	Epoxy		AREMCO 526 N
	Inside diameter of the coil	mm	83.366
	Radial thickness of epoxy surrounding the wire (assumption)	mm	0.051
	Radial thickness/ height of the winding	mm	12.951, 22.007
	Outside diameter (before E-glass wrap)	mm	109.268
	Turn counts per coil		92
	Number of layers (L) of winding		8
	Number of turns per layer		12 (L1,3,5 and 7) 11 (L2, 4,6 and 8)
	Thickness of E-glass wrap on the outer surface of the coil (two layers of 0.1mm thick E-glass tape painted with epoxy)	mm	0.2
	Length of lead wires from the coil	mm	914.4
	Estimated length of copper wire per coil (including lead wires)	m	29.84
Bushing with flange (JL0091130-0318-02)	Material		Rulon
	Inside diameter, outside diameter of the bushing	mm	2.388, 6.198
	Height of the bushing, excluding the top flange	mm	6.477
	Outside diameter, thickness of the flange	mm	11.176, 1.397
Magnet retaining clip (JL0091130-0317)	Material		SS 304
	Overall length, width	mm	25.4, 9.65
	Thickness of the top section (facing coil bobbin), bottom section (facing the CF flange/ mount collar)	mm	3.68, 6.35
MHD Magnet Assembly*	Distance between the opposite pair of coils	mm	174.752
	Number of coils per magnet		4
	The overall dimensions of MHD magnet mounted onto the six-way cross cube assembly	mm	233.53 (width) 233.53 (thickness) 233.53 (height)
Note: *Refer to JL0091130-0304 (Aperture 1 assembly model) and JL0091130-0306 (Aperture 2 assembly model) for details.			

4.2 The MHD coil design is optimized for the use of 14 AWG single-strand, round copper wire with polyimide heavy-build insulation. The resultant dimensions of the single pancake coil and other major components for the magnet assembly (See Figure 2 for details) are given in Table 1. The manufacturing considerations are as follows:

4.2.1 All coils of a given lot shall use the magnet wire from the same production batch.

4.2.2 The coil shall be wet wound clockwise and in hexagonal close pack configuration on the stainless-steel bobbin (label 6 in Figure 2) using a single, uninterrupted length of copper wire and AREMCO® 526 N ultra-high temperature epoxy.

4.2.3 Kapton film provides electrical insulation between the bobbin and the coil: (a) the bobbin core shall be wrapped with 0.254 mm thick Kapton tape; (b) Similarly, 0.254 mm thick pre-cut Kapton spacer shall be used between the flat surfaces of the coil and the top and bottom flanges of the bobbin.

4.2.4 The winding shall begin from the top flange side of the bobbin and complete also at the same side of the bobbin flange to simplify lead wire routing for the electrical termination of the magnet assembly.

4.2.5 Each coil shall contain 92 turns distributed over eight consecutive layers. The odd number of layers shall contain 12 turns per layer, whereas 11 turns per layer shall be present in the even layers of the coil pack. Grooves shall be added to the outside surface of the bobbin core to regulate the winding pattern of the coils. All coils in a given lot shall have identical turn counts.

4.2.6 The leads shall be 36 inches (914.4 mm) long.

4.2.7 G-10 shim shall be used to fill the void and to allow a smooth transition of the wire between the neighboring layers of the winding pack.

4.2.8 The lead wires shall exit through the openings (diameter=6.35 mm) made on the top flange of the bobbin. The openings shall contain Rulon bushing (Table 1) to provide an insulating barrier between the lead wire and the top flange and strain relief for the section of the lead wire close to the winding pack.

4.2.9 The outer surface of the winding pack shall be wrapped under tension with two layers of 0.1 mm thick E-glass cloth and painted subsequently with AREMCO® 526 N epoxy. The same epoxy shall be used to secure the Rulon bushing in place on the top flange of the bobbin and to fill space between the lead wire and the inside surface of the bushing. The excess epoxy shall be carefully removed before curing the coils.

4.2.10 The finished wet coil shall be baked in the oven at 93.3°C for 3 hours followed by 2 hrs at 162.8°C.

4.2.11 The lead wires shall be protected against damage during the coil manufacturing process.

4.2.12 The lead wire shall be and dressed with a fiberglass fabric sleeve. The bottom-most section of the lead wire shall be reinforced further with 3M 361 glass cloth tape with silicone adhesive.

4.2.13 The lead wires shall be labeled, trimmed as needed, and terminal lugs shall be crimped onto the lead end.

4.3 The bottom flange of the bobbin contains additional mechanical features to level the coil-bobbin assemblage above the bolted CF flanges (label 9 in Figure 2) and the mounting collar (label 10 in Figure 2) attached to the CF six-way cross cube assembly.

4.4 The four-pancake coil-bobbin assemblies are firmly held against the CF flanges and mounting collar fitting of the 6-way cross cube by the four retaining clips with fasteners for each coil unit. The assembly is such that the distance between the opposite pair of coils for the vertical and horizontal steering corrector assembly is 174.75 mm. See Table 1 for the overall dimensions of the MHD magnet.

5 As-Built Coil Parameters

Technicoil Inc. USA procured the magnet wire from Rea Magnet Wire Company Inc., USA, and fabricated the coil and bobbin as per the drawings (Table 3) and specification (section 4 of this document) supplied by J Lab. Table 2 shows the actual dimensions of the copper wire and the average dimensions of the coils fabricated by this vendor. The coil winding machine parameters are set to achieve 95 turn counts in the coil spanning 8 layers of winding.

Table 2: The nominal dimensions of the magnet wire and the coils fabricated for the MHD steering corrector magnet.

Parameter	Unit	Value
Magnet Wire (Supplier: Rea Magnet Wire Company Inc. USA)		
Bare wire diameter	mm	1.63
Insulated wire diameter	mm	1.676
MHD Coils (Manufacturer: Technicoil Inc. USA)		
Turn counts per coil		95
Inside diameter (average value)	mm	83.363
Outside diameter (excluding E-glass wrap) (average value)	mm	118.194
Height of the coil winding (average value)	mm	22.15
Length of lead wire	mm	915
Length of the copper per coil (including lead wires)	m	~31

We procured twelve coils, eight of them are used to assemble two MHD magnets installed in the A1 and A2 girder assembly. The remaining four coils will be used in the spare assembly. All coils of this lot have identical turn counts (Table 2). The measured values of bobbin dimensions agree well with the original specification (Table 1) and are within the fabrication tolerance specified in the corresponding CAD drawing (item 1 in Table 3).

Table 3: Applicable CAD drawings (PDF) based on the new design of the MHD magnet.

	Reference number	Description
1	JL0091130-0318-01	MHD coil bobbin
2	JL0091130-0318-02	MHD bushing
3	JL0091130-0318	MHD coil assembly

6 Electrical Wiring Diagram

The EM simulation models and the magnetic testing follows the electrical wiring diagram as shown in Figure 3. The MHD magnet is installed in the girder assembly with the lead wires point to downstream of the beam trajectory (+Z –axis). The top right panel shows the pair of lead wires from each coil pack.

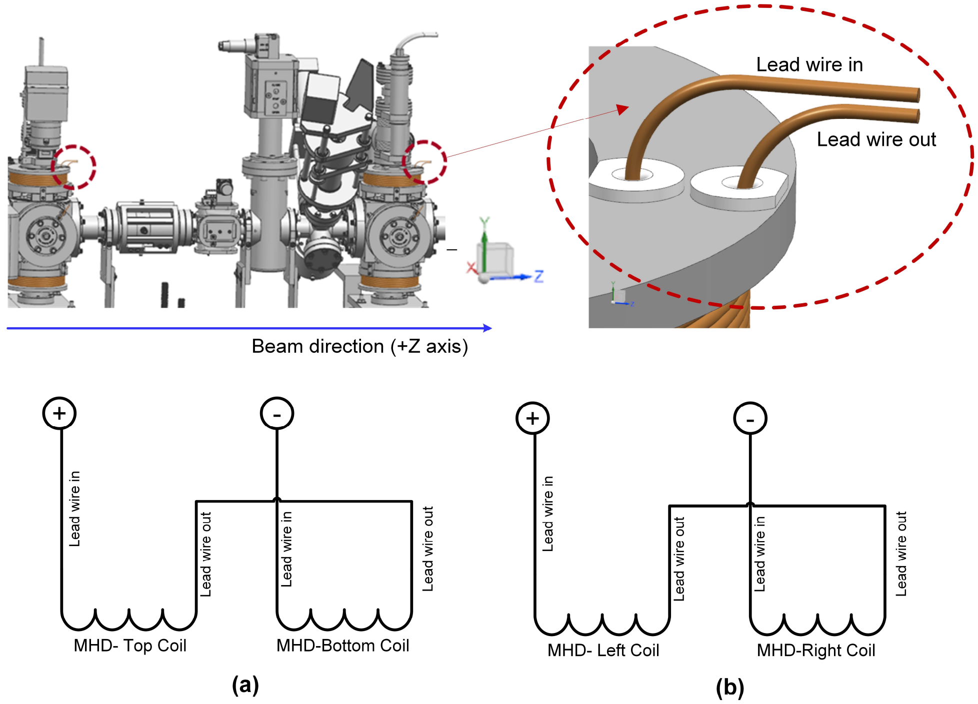

Figure 3: Electrical wiring diagram for the (a) MHD vertical dipole coil assembly, and (b) MHD horizontal dipole coil assembly. The magnet is positioned in the girder assembly such that the coil lead wires point to the downstream side of the beam trajectory as shown in the top left panel of the figure. The right panel shows a closer view of the top flange of the coil bobbin where the lead wires exit from the coil pack.

7 Results and Discussions

7.1 Table 4 shows the magnetic performance parameters of the MHD vertical or horizontal dipole coil assembly energized separately to achieve the maximum integrated dipole field strength of 5.5×10^{-5} T.m along the longitudinal axis and in the good field region with a 4 mm radius. As per the primary design specification (see the notes in the first row of Table 4), the vertical or horizontal dipole coil assembly, with 92 turn counts per coil, needs to be energized at 2.535 A to yield the required maximum integrated dipole field strength, whereas the performance validation studies indicate that the actual assembly with 95 turn counts per coil, requires 2.8 A to meet the same requirements.

7.2 The coils are designed with a sufficient safety margin (both operating current and temperature). For instance, the anticipated temperature of the coil at 4 A is ~37°C. 10 A trim card power supply will be used to energize the MHD magnet assembly in the beamline.

7.3 As shown in Figure 4, the inner windings of the coil pack experience the highest field strength at any given excitation current. For example, the peak field in the production coil

Approved: 05/13/2021; E-Sign ID: 439499; Signed By: Reviewer 1: J. Grames; Reviewer 2: M. Stutzman; DCG Quality Check: T.

increases at a rate of 2.43 mT/A which corresponds to 6.8 mT at 2.8 A for the MHD vertical and horizontal dipole coil assemblies. Figure 5 shows the overall field distribution (including the fringe fields) at the transverse mid-plane (XY plane, Z=0) of the vertical dipole assembly.

Table 4: Magnetic performance parameters at the maximum operating conditions of the vertical (V) or horizontal (H) dipole coil assemblies in the MHD steering corrector magnet.

Parameter	**Unit**	**Value**	
ANSYS Maxwell case studies		**Based on the primary design model** *(See Table 1 for coil and bobbin model parameters)*	**Based on the performance validation model** *(See Table 2 for the production coil model parameters and Table 1 for coil bobbin parameters)*
MHD dipole coil assembly configuration		Vertical (V)/ Horizontal (H)	Vertical (V)/Horizontal (H)
Reference radius (R_{ref})	mm	4	4
Max. operating current of the coil (I_{max})	A	2.535	2.8
Operating current density in the copper wire	A/mm^2	1.12	1.34
The maximum field strength in the coil pack	mT	6.45	6.8
Integrated dipole field strength along the longitudinal axis and at R_{ref} of the horizontal MHD-V or MHD-H dipole coil assembly $\left(\int_{z=-1m}^{z=+1m} B_{n=1}(r = R_{ref}, z).dz\right)$	T.m	5.51×10^{-5}	5.50×10^{-5}
Effective magnetic length (L_{eff}) of the horizontal MHD-V or MHD-H dipole coil assembly	m	0.107	0.0901
Integrated strength along the longitudinal axis and at R_{ref} of sextupole field component of the horizontal MHD-V or MHD-H dipole coil assembly $\left(\int_{z=-1m}^{z=+1m} B_{n^*=3}(r = R_{ref}, z).dz\right)$	T.m	-2.06×10^{-7}	-2.49×10^{-7}
Dipole integrated field quality at R_{ref}	%	99.63	99.55
The magnetic stored energy of the MHD-V or MHD-H dipole coil assembly at I_{max}	mJ	6.32	8.24
Total Inductance of the MHD-V or MHD-H dipole coil assembly at I_{max}	mH	1.97	2.10
The resistance of the MHD single pancake coil at 20°C.	Ω	0.24	0.25
Cumulative strength of Lorentz force (F_{cum}) at I_{max} in the single pancake coil	mN	0.9	1.3

(a)

(b)

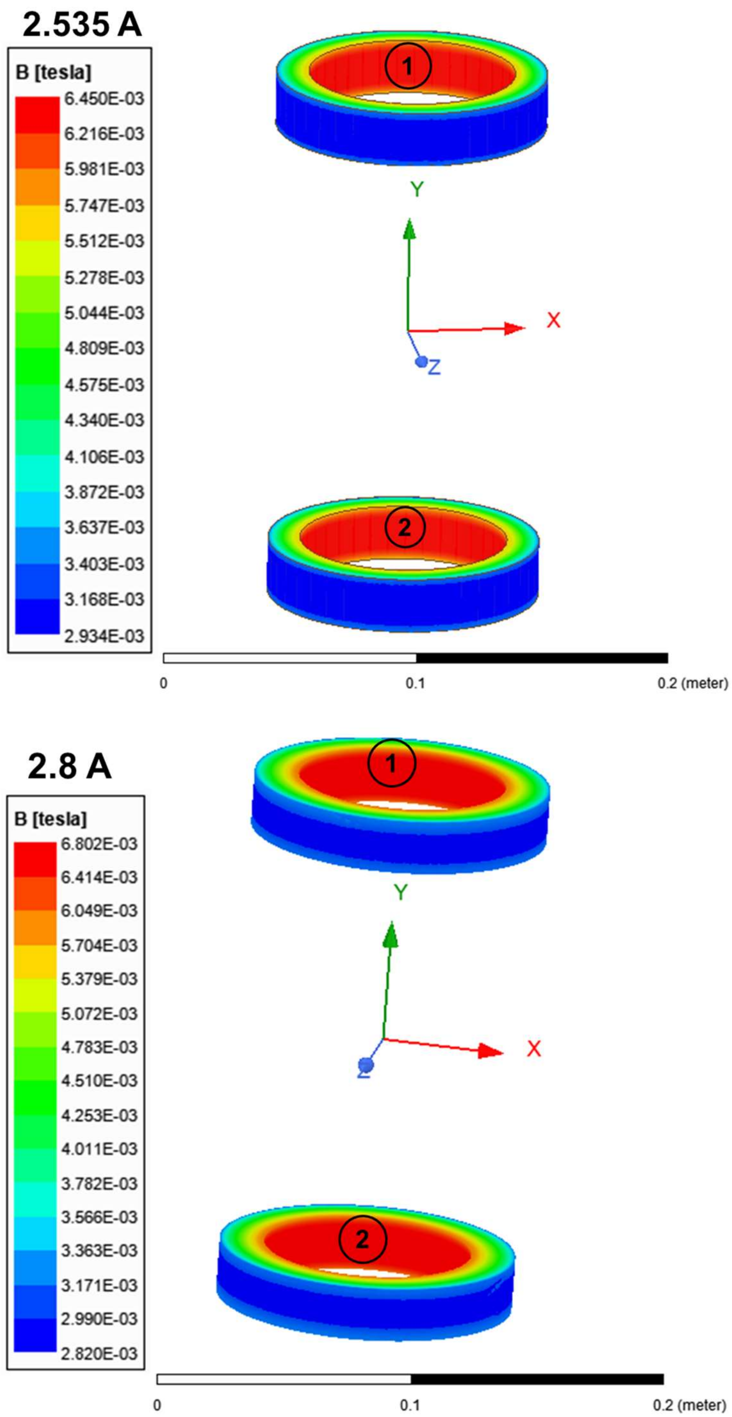

Figure 4: The magnetic field distribution at the maximum operating conditions of the MHD vertical dipole coil assembly at (a) 2.535 A (see Table 1 for the primary design specification), and (b) 2.8 A (see Table 2 for the nominal dimensions of the coils fabricated for the MHD magnets in the A1 and A2 aperture cube assemblies). Labels 1 and 2 denote the top and bottom coils in the MHD magnet assembly as shown in Figure 2.

(a)

(b)

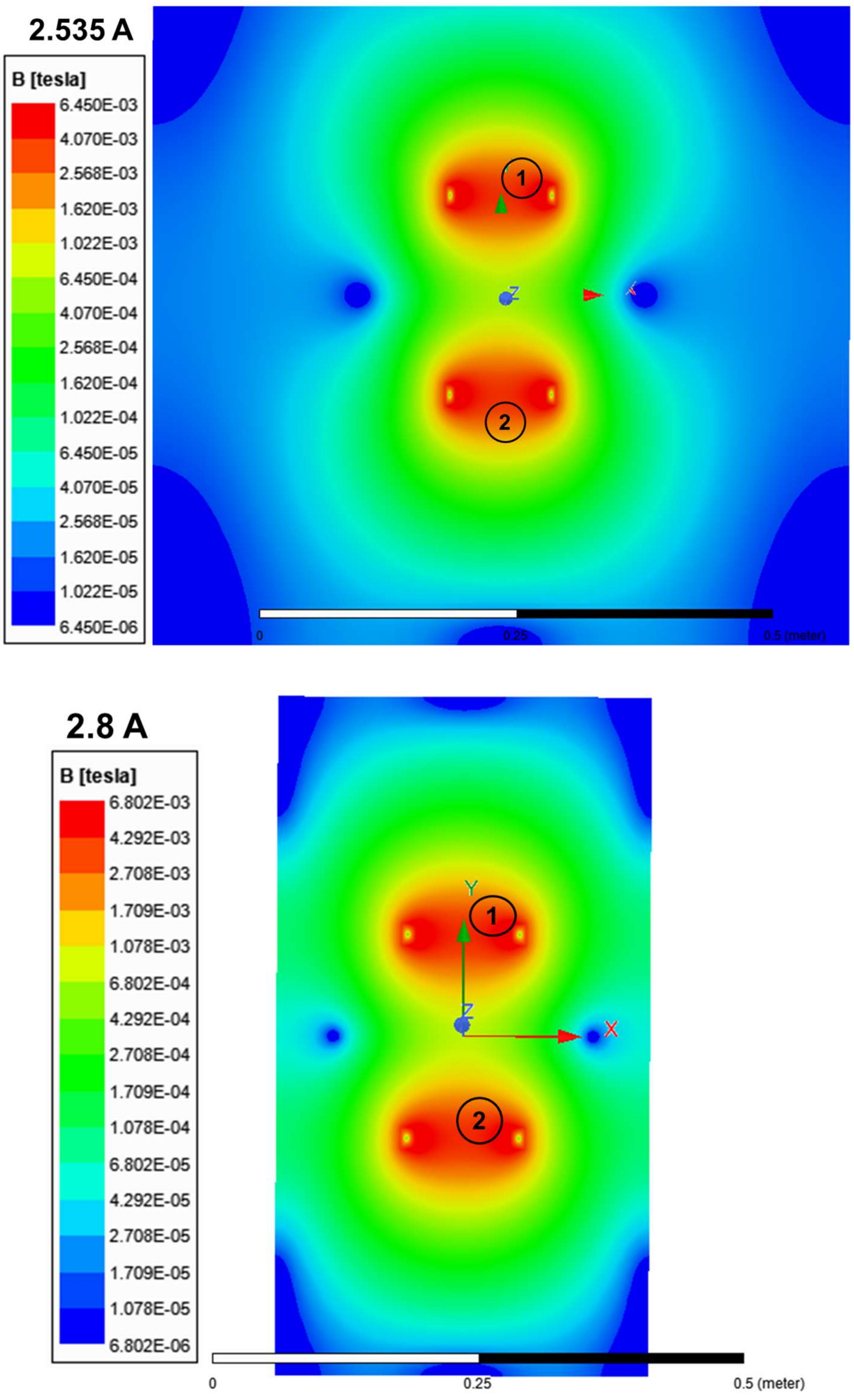

Figure 5: The magnetic field distribution at the mid-plane (XY plane, Z = 0) of the MHD vertical dipole coil assembly at (a) 2.535 A (see Table 1 for the primary design specification), and (b) 2.8 A (see Table 2 for the nominal dimensions of the coils fabricated for the MHD magnet in the A1 and A2 aperture cube assemblies). Labels 1 and 2 denote the top and bottom coils in the MHD magnet assembly as shown in Figure 2.

(a)

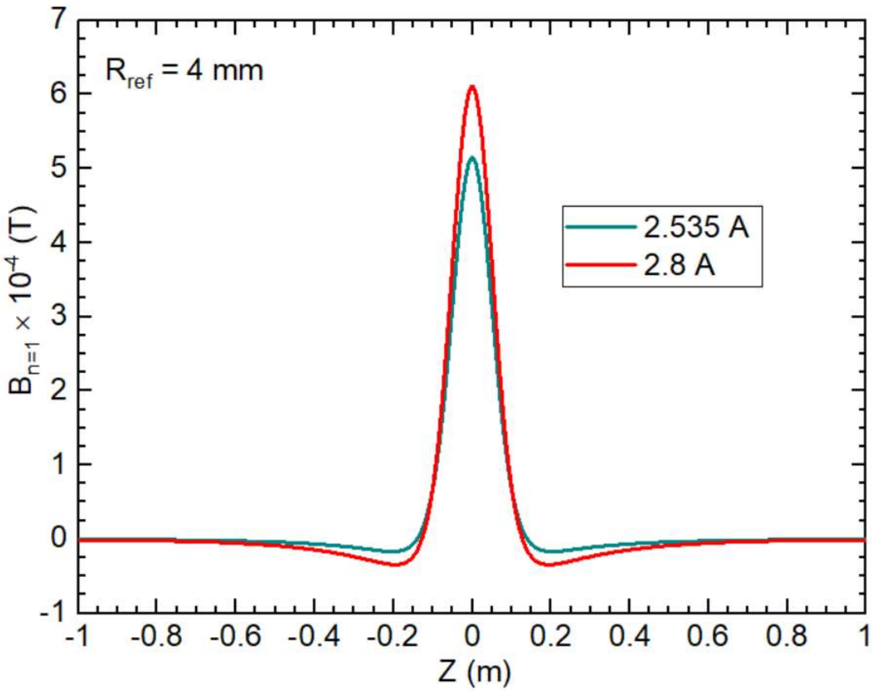

(b)

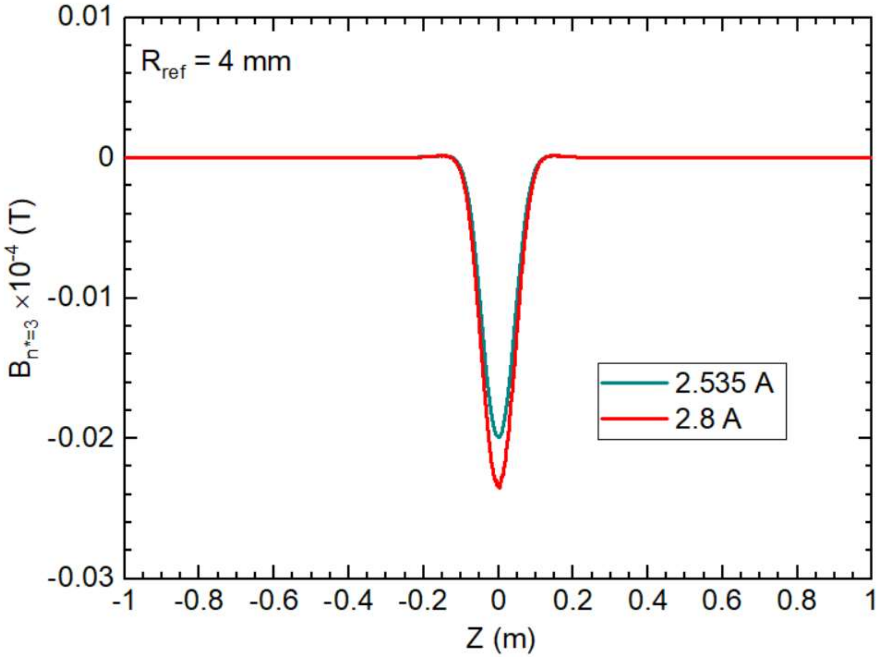

Figure 6 (a) The main dipole field ($B_{n=1}$) and (b) the sextupole harmonic field ($B_{n^*=3}$) profile along the longitudinal axis (Z-axis) of the MHD vertical dipole coil assembly at 2.535 A (as per the primary design model in Table 1) and 2.8 A (model based on the as-built coil parameters in Table 2). The field values are at a distance of 4 mm radially (R_{ref}= 4 mm) from the magnet center (Z = 0).

The Design Report of MHD Steering Corrector Magnet in the CEBAF 200 keV Injector Beamline

(a)

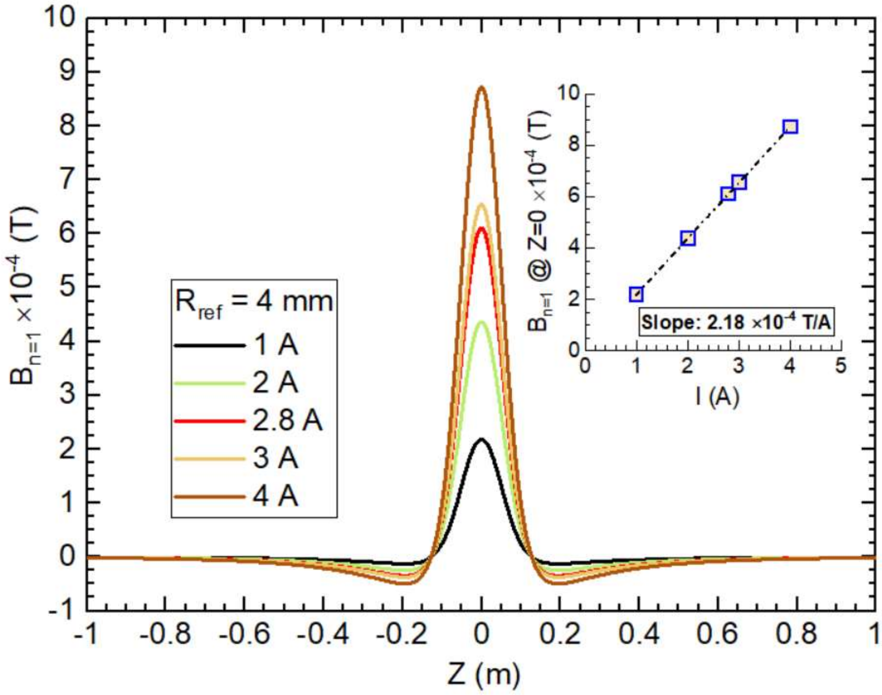

(b)

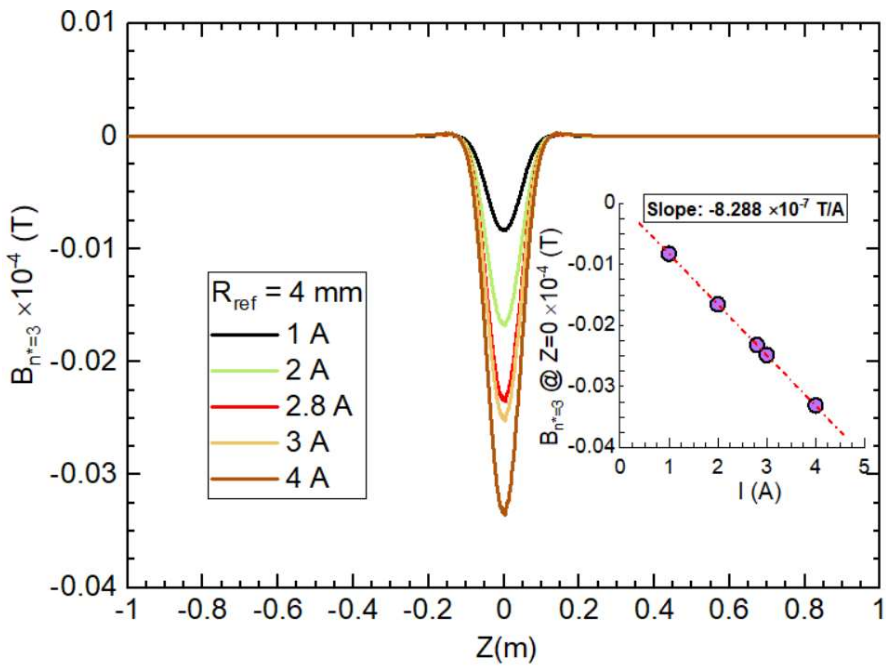

Figure 7: The main dipole field ($B_{n=1}$) and (b) the sextupole harmonic field ($B_{n^*=3}$) profile along the longitudinal axis (Z-axis) of the MHD vertical dipole coil assembly. These data are obtained from the 3D EM simulation of the MHD magnet model based on the as-built coil parameters as shown in Table 2. The field values are at a distance of 4 mm radially (R_{ref}=4 mm) from the magnet center (Z = 0) and for the coil excitation currents (I) up to 4 A. The dotted lines in the inset figures represent the linear fit of the peak field values for I ≤ 4 A.

(a)

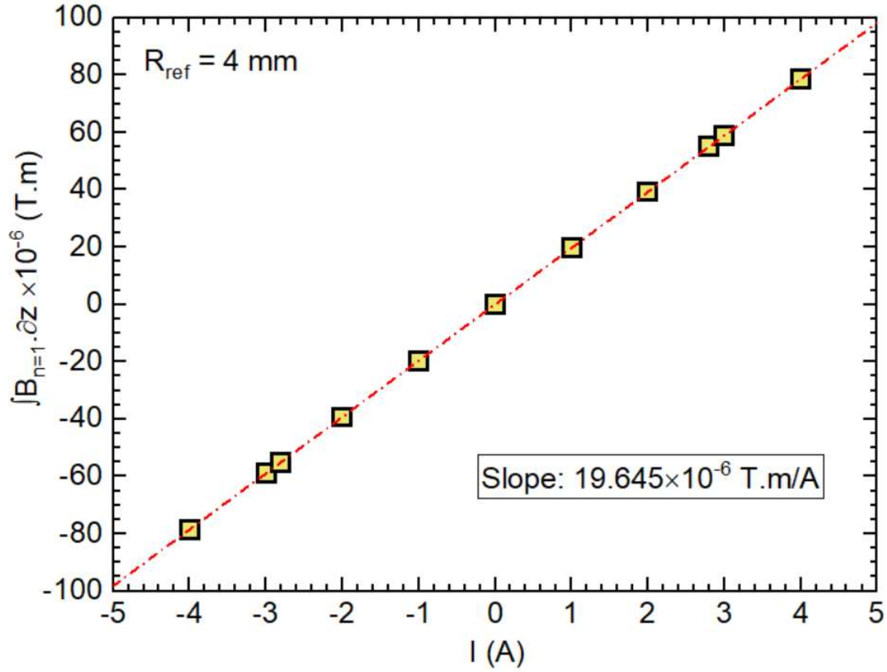

(b)

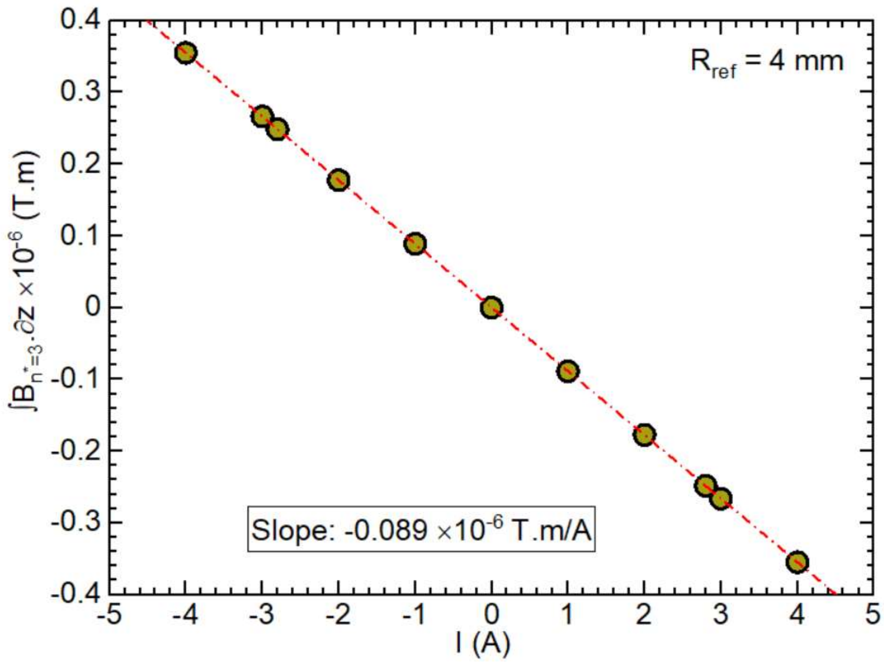

Figure 8: The solid symbols represents (a) the integrated dipole field strength and (b) the sextupole harmonic field strength at R_{ref}=4 mm with coil excitation current ≤ 4A of the MHD-vertical/ horizontal dipole coil assembly. These data are obtained from the 3D EM simulation of the MHD magnet model according to the as-built coil parameters as shown in Table 2. The dot-dash line represents the linear fit to the data plotted in the same figure.

(a)

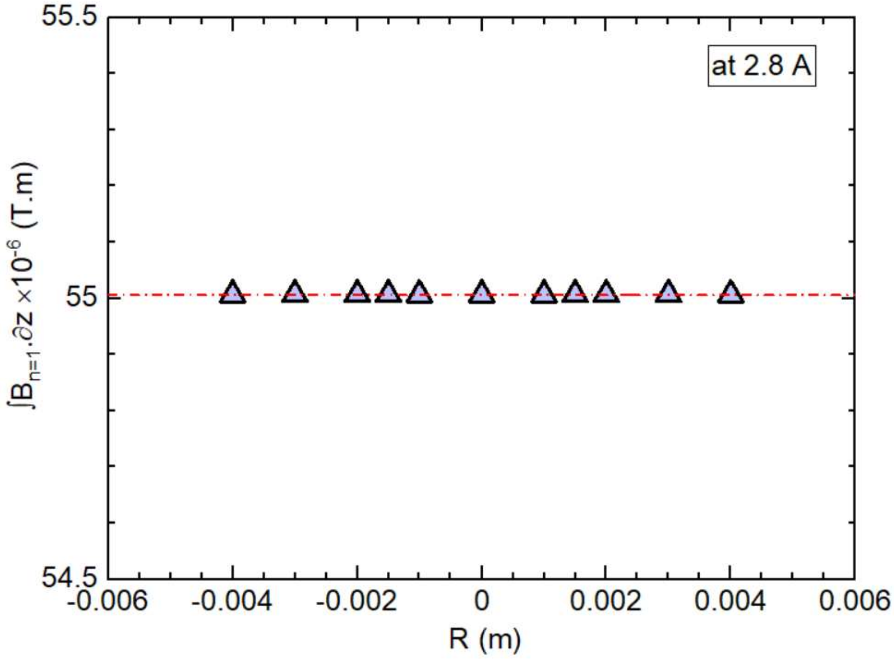

(b)

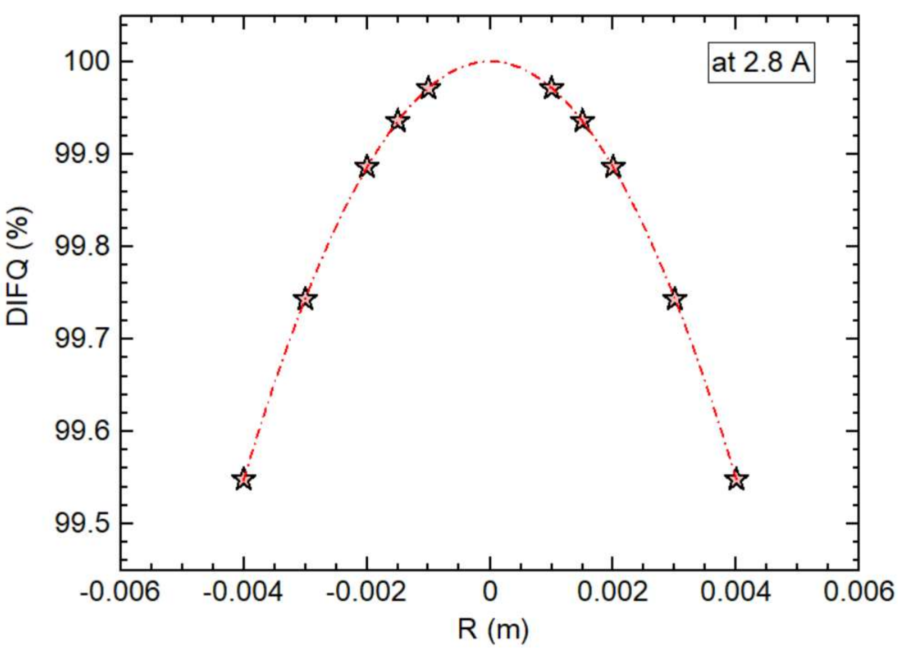

Figure 9: The solid symbols show (a) integrated dipole field strength and (b) dipole integral field homogeneity within the good field region of the MHD vertical/ horizontal dipole coil assembly. These data are obtained from the 3D EM simulation at 2.8 A of the MHD magnet model according to the as-built coil parameters as shown in Table 2. The dot-dash line represents the fit curve to the data plotted in the same figure.

Table 5: Integrated dipole field strength as a function of the operating current (±4 A) for the vertical (V) or horizontal (H) dipole coil assemblies in the MHD steering corrector magnet. The data is obtained from the 3D EM simulation of the as-built coil models. See Table 2 for the coil parameters.

Operating current (A)	Integrated dipole field strength $\times 10^{-6}$ (T.m)
4	78.580
3	58.935
2	39.290
1	19.645
0	0.000
-1	-19.645
-2	-39.290
-3	-58.935
-4	-78.580

Table 6: The inductance matrix of the vertical (V) or horizontal (H) dipole coil assemblies in the MHD steering corrector magnet. The data is obtained from the 3D EM simulation of the as-built dipole assembly coil models. See Table 2 for the coil parameters.

MHD-Vertical dipole coil assembly (Unit: H)		
	Coil-Top	Coil-Bottom
Coil-Top	1.04E-03	1.06E-05
Coil-Bottom	1.06E-05	1.04E-03

MHD-Horizontal dipole coil assembly (Unit: H)		
	Coil-Left	Coil-Right
Coil-Left	1.04E-03	1.06E-05
Coil-Right	1.06E-05	1.04E-03

7.4 The multipole field analysis results of the MHD dipole coil assembly suggest that the field errors are solely due to its first higher-order harmonics, sextupole field component. See Figure 6 and Figure 7 for details. The overall strength of the sextupole field component at $R_{ref} = 4mm$ is two orders of magnitude smaller than the leading dipole field component.

7.5 The peak strength of the main dipole field component of the production coil assembly increases at a rate of 2.18×10^{-4} T/A, whereas the similar value for the sextupole field component is -0.0083×10^{-4} T/A.

7.6 The integrated dipole field strength and integrated sextupole field strength of the production coil assembly at $R_{ref} = 4mm$ varies respectively at a rate of 19.645×10^{-6} T.m/A and -0.089×10^{-6} T.m/A (Figure 8). The dipole integral field strength is uniform and the calculated value of the integrated dipole field uniformity in GFR is better than 99.55 % (Figure 9). The effective magnetic length is 0.090 m. Table 5 lists the dipole field integral strength as a function of coil excitation current up to 4 A. These data will be used in the CEBAF machine control system.

7.7 The inductance matrix of the actual dipole coil assemblies is given in Table 6. The inductance calculation is based on the coil turn count provided in Table 2. The number in diagonal from the upper-left to the lower-left corners represents the self-inductances of the coils (1.04 mH) in the vertical/ horizontal dipole coil assembly, whereas the non-diagonal numbers (0.01 mH) signify the mutual inductances between those coils.

7.8 The net force for the vertical dipole coil assembly is dominated by the vertical field component (F_y). The net values of force components in the horizontal (F_x) and longitudinal (F_z) are practically negligible. F_y is tensile in nature. The net cumulative force at 2.8 A is 1.3 mN (Table 4). Similarly, the net forces for the horizontal dipole coil assembly are dominated by the horizontal field component (F_x), similar in magnitude to the F_y component for the vertical dipole coil assembly. The coils are held in place in the assembly with the magnet retainer clips (label 7) as shown in Figure 2. The overall geometry and dimensions of the magnet retainer clip are based on the structural analysis using the Lorentz force data for the MHD magnet assembly.

8 Test Plan

The magnet measurement facility presently has the test set up to perform the magnetic profile measurements using only a uni-axial hall probe. The magnetic field measurement plan is provided in section #8.3. These data will be compared against the EM simulation results of the vertical dipole coil assembly model based on the production coil parameters (Figure 10 and Figure 11). Multipole field analysis of the EM simulation data will be used to extract the relevant physics parameters for the magnet system and to provide data to the CEBAF machine control system.

8.1 Quality Assurance tests

8.1.1 Perform the visual inspection and record the observations.

8.1.2 Record the wire dimensions at three pre-selected locations of the two lead wires and note down the average value.

8.1.3 Record the room temperature resistance of the coil (note down the ambient conditions)

8.1.4 Record the coil inductance at 60 Hz.

8.1.5 Hipot and surge test at 500 V; leakage current should be less than 5 μA.

8.1.6 Record the temperature evolution of one representative coil energized at 2.5 A and 4 A. Monitor the readings at least for four hours.

8.2 Assemble one pair of coils (top and bottom) on the spare CF 6-way cross assembly. Dress the lead wires. Complete the electrical wiring connections. Record the room temperature resistance of the vertical dipole coil assembly.

8.3 Magnetic field measurements of the vertical dipole coil assembly.

8.3.1 Measure vertical field (B_y) versus Z at X-values indicated below and at I=0 with coils and cube assembly (background measurements)

8.3.1.1 Z range: ±0.5 m from the magnet center.

8.3.1.2 Z step: at 10 mm interval from Z=-0.5 m to -0.3 m; at 2 mm interval from Z=-0.3 m to +0.3 m; at 10 mm interval from Z=0.3 m to 0.5 m.

8.3.1.3 X= 4 mm and 0 mm (X denotes the horizontal distance from the magnet center).

8.3.2 Measure $B_y\ (Z)$ at X= -4 mm and X=0 mm at I=±4 A.

8.3.2.1 Z range: ±0.5 m from the magnet center.

8.3.2.2 Z step: at 10 mm interval from Z=-0.5 m to -0.3 m; at 2 mm interval from Z=-0.3 m to +0.3m; at 10 mm interval from Z=0.3 m to 0.5 m.

8.3.3 Measure $B_y\ (Z)$ at X= 0 mm for I values indicated below.

8.3.3.1 Z range: ±0.5 m from the magnet center.

8.3.3.2 Z step: at 10 mm interval from Z=-0.5 m to -0.3 m; at 2 mm interval from Z=-0.3 m to +0.3 m; at 10 mm interval from Z=0.3 m to 0.5 m.

8.3.3.3 I=0 A (background), 1 A, 2 A, 3 A, 4 A, 0 A (repeat the background measurement)

8.3.4 Background measurements (I=0 A) without altering the setup, but after removing the coils from the spare CF 6 way cross cube assembly (i.e background measurements with spare cube assembly only).

8.3.5 Background measurements (I=0 A) without spare cube assembly only (Hall probe scan in free space).

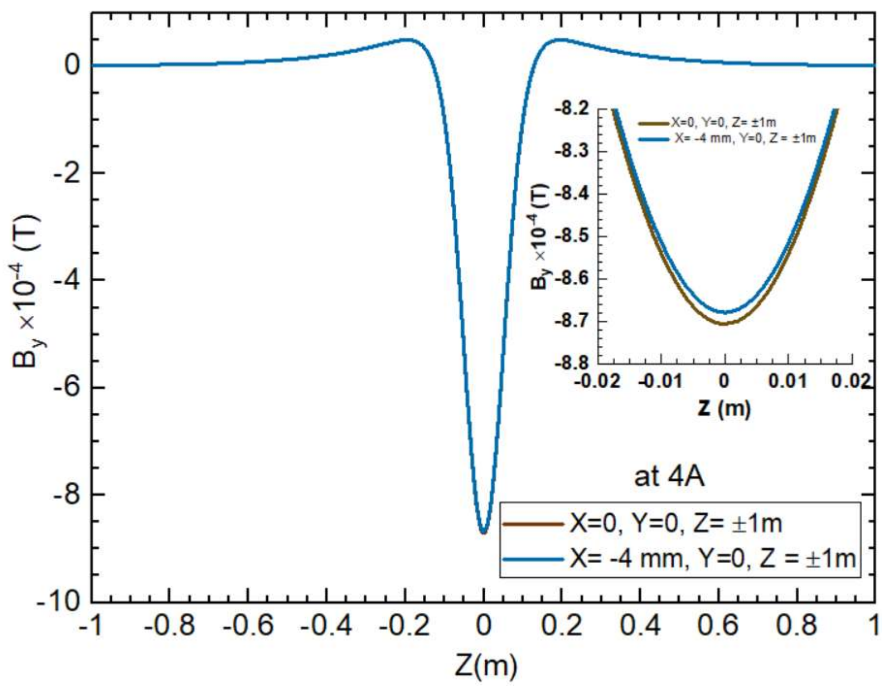

Figure 10: The vertical field (B_y) profile over Z=±1m from the magnet center (X=0, Y=0, Z=0) and (X=-4 mm, Y=0, Z=0) of the MHD vertical dipole coil assembly. This data is obtained from the EM simulation of the MHD magnet model using the production coil parameters listed in Table 2. The coils are energized at 4 A. Refer to Figure 3(a) for the electrical wiring diagram. Inset shows the same data close to the magnet center on an enlarged scale.

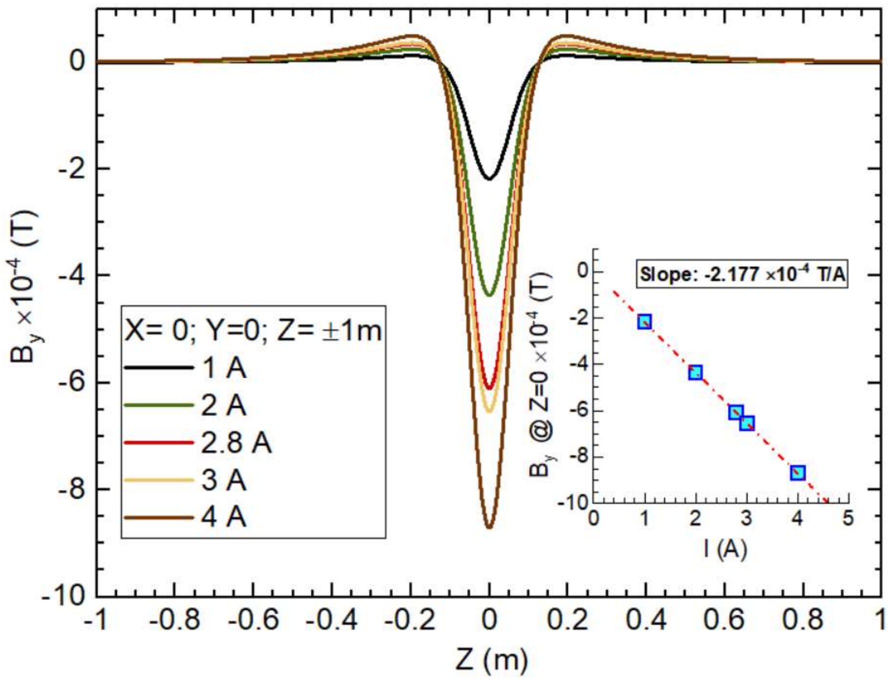

Figure 11: The vertical field (B_y) profile over Z=±1m from the magnet center (X=0, Y-=0, Z=0) of the MHD vertical dipole coil assembly for coil excitation currents ≤ 4A. This data is obtained from the EM simulation of the MHD magnet model using the production coil parameters listed in Table 2 Refer to Figure 3(a) for the electrical wiring diagram. Table 7 lists the integrated strength of the vertical field component over the same Z range and for I≤ ±4 A.

Table 7: Integrated strength of vertical field component as a function of the operating current (±4 A) for the vertical (V) dipole coil assembly in the MHD steering corrector magnet. Figure 11 shows the corresponding $B_y(Z)$ data for I ≤ 4A This data is obtained from the 3D EM simulation of the as-built coil models. See Table 2 for the coil parameters.

Operating current (A)	Integrated strength of vertical field (B_y) component $\times10^{-6}$ (T.m)
4	-78.580
3	-58.935
2	-39.290
1	-19.645
0	0.000
-1	19.645
-2	39.290
-3	58.935
-4	78.580

9 Summary

The electromagnetic-mechanical design analysis and performance validation studies suggest that the new MHD steering corrector magnet for the 200 keV injector beamline meets the overall performance requirements. The coils are designed with a sufficient safety margin. The magnet will require a 10 A power supply. The magnetic analysis results indicate the field errors are due to the first allowed harmonics, the 6 pole field component. The integrated field strength of the 6 pole field component is two orders of magnitude smaller than that of the leading dipole field component. The integrated field homogeneity in the good field region with a radius of 4 mm is better than 99.55 %. The maximum operating current is set to 4 A in order to keep the coil temperature below 40°C during the continuous operation in the beamline. All components used in the coils and magnet assembly can withstand a maximum of 200°C to comply with the bake-out procedure for the beamline vacuum components.

10 References

[1] J Lab Drawing ACC0002845-0001: ACC Machine configuration- Beam transport injector.

[2] J Lab 3D NX CAD Model JL0091130-0300-Section 03. VBV1I07 TO VBV0I02

[3] J Lab 3D NX CAD Model JL0091130-0304: Aperture 1 assembly.